Journal of
Mechanics of
Materials and Structures

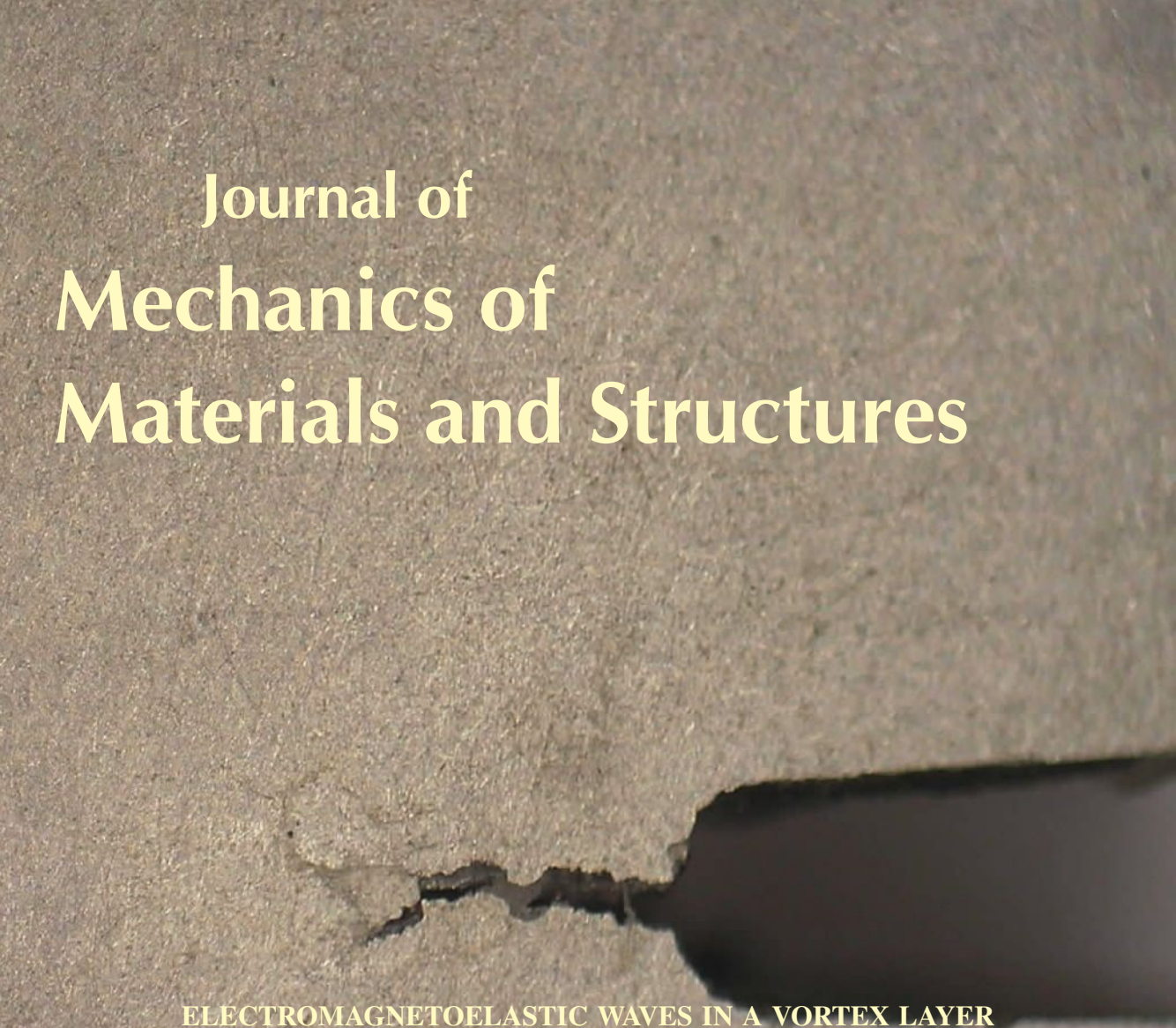

ELECTROMAGNETOELASTIC WAVES IN A VORTEX LAYER OF A SUPERCONDUCTOR

Bogdan T. Maruszewski, Andrzej Drzewiecki and Roman Starosta

Volume 7, No. 3 March 2012

msp

JOURNAL OF MECHANICS OF MATERIALS AND STRUCTURES
Vol. 7, No. 3, 2012
dx.doi.org/10.2140/jomms.2012.7.297

ELECTROMAGNETOELASTIC WAVES IN A VORTEX LAYER OF A SUPERCONDUCTOR

BOGDAN T. MARUSZEWSKI, ANDRZEJ DRZEWIECKI AND ROMAN STAROSTA

Magnetic field enters the type-II superconducting body along a discrete arrangement of magnetic vortex lines. The paper aims at investigating the dispersion and amplitude distributions of magnetoelastic waves propagating solely in the vortex field of the superconducting layer. Our attention has been focused on the dispersion features and amplitudes for various wave velocities. The vortex field consists only of soft vortices (the superconducting crystal is free of lattice defects).

1. Introduction

Magnetic flux can penetrate the type-II superconductor in the form of Abrikosov vortices (also called flux lines, flux tubes or fluxons), each carrying a quantum of magnetic flux. Since the vortices are formed by the applied magnetic field, the supercurrent flows around of each of them. There exist also Lorentz force interactions among them, which give rise to an additional thermomechanical (stress) field in type-II superconductors. Near the lower critical magnetic intensity limit H_{c1}, this field has elastic character. However, if the density of the supercurrent is above its critical value and/or the temperature is sufficiently high, there occurs a flow (creep or diffusion) of vortex lines in the superconducting body. The *fluidity* of the vortex array has been also observed when the applied magnetic field approaches its upper critical limit H_{c2} [Blatter et al. 1994; Brandt 1995; Cyrot and Pavuna 1992]. Following a magnetothermomechanical model of interactions in such II-type superconductors both for the *lattice-like* and *fluid-like* states of the vortex field, where the specific definition of the vortex field stress tensor has been introduced [Maruszewski 1998; 2007], this paper aims at determining the dispersion and amplitude distributions of magnetoelastic waves propagating along soft vortices in the superconducting layer.

If the crystal lattice of the layer is free of lattice defects, there is a parallel arrangement of soft vortex cores (Figure 1, left). However, in real crystals, imperfections such as vacancies, dislocations, disclinations, grain boundaries, and interstitial atoms cause that the vortex lines can be curved or even tangled because of pinning (Figure 1, right). We have confined in the paper only to the *lattice-like* state. The choice of the geometry of the vortex field (layer) was motivated by a need to check if those magnetoelastic waves and electromagnetoelastic waves in such peculiar environment are possible to be guided.

The natural conditions where devices may use such a technological solution exist in space where temperature is about 4K and majority of elements and materials behave as superconductors. In the paper the particular analysis of the SH magnetoelastic and compressional and flexural electromagnetoelastic modes has been presented.

Partially supported by Poland's Ministry of Science and Higher Education (MNiSzW) grant 1101/T02/2006/30 and DS grant 21-320/2009.
Keywords: magnetoelastic waves, dispersion, superconductor.

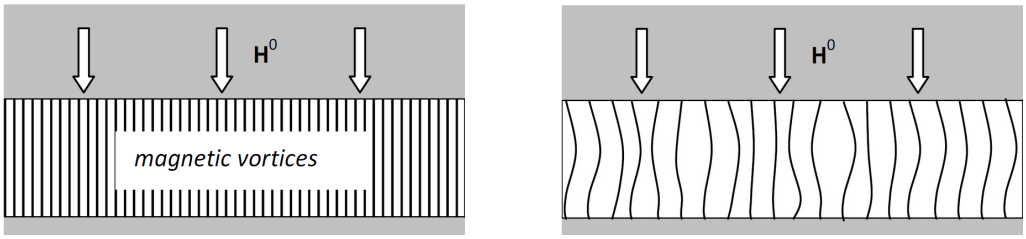

Figure 1. Vortices in a perfect crystal (left) and in a real one (right), where pinning can occur.

2. General wave equations

Let us now consider a problem which deals with the dynamics of the previously defined vortex field. Following the thermodynamical model of the electromagnetomechanical interactions in continuous media, i.e., the momentum balance with Hooke's law and the Maxwell equations in the moving frames with the first London equation we are able to formulate proper equations describing dynamics of the vortex field in the elastic superconductor. For the sake of simplicity thermal influences have been omitted. The governing equations of the electromagnetoelastic vortex waves read as follows [Maruszewski et al. 2007]:

$$\begin{aligned} \mu u_{i,jj} + \eta \dot{u}_{i,jj} + (\lambda+\mu) u_{j,ij} + \tfrac{1}{3}\eta \dot{u}_{j,ij} - \mu_0 (h_{r,i} - h_{i,r}) H_r^0 - \rho \ddot{u}_i = 0, \\ \lambda_0^2 h_{i,kk} - h_i + u_{i,k} H_k^0 - u_{k,k} H_i^0 = 0, \\ \lambda_0^2 e_{i,jj} - e_i + \mu_0 e_{ijk} \dot{u}_j H_k^0 = 0, \end{aligned} \tag{1}$$

where u_k is the displacement vector of the vortex field point, H_r^0 is the applied magnetic field normal to the limiting surfaces of the layer (Figure 1), h_r is the small contribution to the total magnetic field in the layer comparing to H_r^0 and describes its perturbations, because the linear form of equations (1) results from

$$H_k = H_k^0 + h_k, \quad |h_k| \ll |H_k^0|. \tag{2}$$

Here e_k is the electric field intensity understood in the sense of (2), λ and μ are Lamé's constants, μ_0 is the permeability of vacuum, η is the viscosity coefficient (inside each vortex core flows a normal current, so the Ohmic resistivity occurs there [Cyrot and Pavuna 1992]), ρ is the vortex density [Maruszewski 2007; Maruszewski et al. 2007], and λ_0 is the London penetration depth. Any thermal influences on the considered waves have been omitted. The solutions of equations (1) are looked for in the form

$$f(x_1, x_3, t) = \tilde{f}(x_1) \exp[i(\omega t - k x_3)], \tag{3}$$

where $\tilde{f}(x_1)$ are the amplitudes of signals $u_1, u_2, u_3, h_1, h_2, h_3, e_1, e_2, e_3$ propagating in x_1 direction with the velocity $\boldsymbol{v}$:

$$\tilde{f}(x_1) = \{u_1, u_2, u_3, h_1, h_2, h_3, e_1, e_2, e_3\} \tag{4}$$

if the geometry of the problem is as shown in Figure 2.

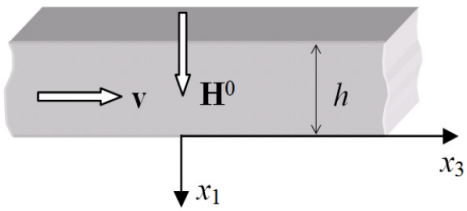

Figure 2. Geometry of the problem.

To facilitate the analysis of the waves, all the relations will be presented in the dimensionless form, with the help of the following substitutions, where $\tilde{c}$ is the speed of light:

$$
\begin{aligned}
&x_1 = hx, \quad x_2 = hy, \quad x_3 = hz, \quad t = T\tau, \quad T = \frac{h}{v_T}, \quad v_T = \sqrt{\frac{\mu}{\rho}}, \quad \Omega = \omega T,\\
&c = \frac{kv_T}{\omega} = \frac{v_T}{v}, \quad \tilde{\lambda}_0 = \frac{\lambda_0}{h}, \quad \tilde{\mu} = \frac{K}{\mu},\\
&K = \lambda + \tfrac{2}{3}\mu, \quad \tilde{\lambda} = \frac{\lambda}{\mu}, \quad \tilde{\rho} = \frac{\rho v_T^2}{\mu} = 1, \quad H^0 = H_{c1}H_0, \quad E = \tilde{c}\mu_0 H_{c1},\\
&c_1 = \frac{v_T}{\tilde{c}}, \quad u_1 = hu_x, \quad u_2 = hu_y, \quad u_3 = hu_z,\\
&\tilde{\eta} = \eta\frac{h}{v_T}, \quad e_1 = Ee_x, \quad e_2 = Ee_y, \quad e_3 = Ee_z, \quad \bar{\mu} = \frac{\mu_0 H_{c1}^2}{\mu},\\
&h_1 = H_{c1}h_x, \quad h_2 = H_{c1}h_y, \quad h_3 = H_{c1}h_z.
\end{aligned}
\tag{5}
$$

3. SH magnetoelastic waves

Let us consider at the beginning the SH magnetoelastic wave propagating along the vortex layer shown in Figure 2. The general equations (1) in this case reduce to

$$\mu u_{i,jj} + \eta\dot{u}_{i,jj} + (\lambda+\mu)u_{j,ij} + \tfrac{1}{3}\eta\dot{u}_{j,ij} - \mu_0(h_{r,i} - h_{i,r})H_r^0 - \rho\ddot{u}_i = 0, \tag{6}$$

$$\lambda_0^2 h_{i,kk} - h_i + u_{i,k}H_k^0 - u_{k,k}H_i^0 = 0, \tag{7}$$

since the SH wave amplitudes in the layer are now looked for in the form (3) with

$$\tilde{f}(x_1) = \{u_2, h_2\}, \tag{8}$$

because

$$\boldsymbol{u} = [0, u_2, 0], \quad \boldsymbol{h} = [0, h_2, 0]. \tag{9}$$

Taking (5) into account, the SH wave equations (6) and (7) become in dimensionless form

$$
\begin{aligned}
(\tilde{\mu} + i\Omega\tilde{\eta})\frac{d^2u_y}{dx^2} + \frac{\Omega^2}{c^2}(v^2\tilde{\rho} - \tilde{\mu} - i\Omega\tilde{\eta})u_y + \bar{\mu}H_0\frac{dh_y}{dx} = 0,\\
\tilde{\lambda}_0^2\frac{d^2h_y}{dx^2} - (\tilde{\lambda}_0^2\frac{\Omega^2}{c^2} + 1)h_y + H_0\frac{du_y}{dx} = 0.
\end{aligned}
\tag{10}
$$

On using relations (5) in (8), the solutions of (10) determine the following amplitudes of the SH magnetoelastic waves:

$$\begin{aligned} u_y &= S_1 e^{p_1 x} + S_2 e^{-p_1 x} + S_3 e^{p_2 x} + S_4 e^{-p_2 x}, \\ h_y &= -M(p_1, \Omega, c) S_1 e^{p_1 x} + M(p_1, \Omega, c) S_2 e^{-p_1 x} - M(p_2, \Omega, c) S_3 e^{p_2 x} + M(p_2, \Omega, c) S_4 e^{-p_2 x}, \end{aligned} \tag{11}$$

where

$$M(p_k, \Omega, c) = \frac{p_k}{\bar{\mu} H_0} + \frac{\Omega^2 (1 - 1/c^2)}{\bar{\mu} H_0 p_k}, \quad k = 1, 2.$$

The parameters p_1 and p_2 were determined from the characteristic equation

$$\tilde{\lambda}_0^2 A(\Omega) p^4 + \left[\tilde{\lambda}_0^2 B(\Omega, c) - F(\Omega, c) A(\Omega) - \mu_0 H_0^2\right] p^2 - F(\Omega, c) B(\Omega, c) = 0 \tag{12}$$

where

$$A(\Omega) = 1 + i\Omega\tilde{\eta}, \quad B(\Omega, c) = \frac{\Omega^2}{c^2}(c^2 - 1 - i\Omega\tilde{\eta}), \quad F(\Omega, c) = \tilde{\lambda}_0^2 \frac{\Omega^2}{c^2} + 1.$$

A detailed analysis of the characteristic equation shows that wave propagation is possible only if

$$B(\Omega, c) > 0. \tag{13}$$

From (13) we get that if SH magnetoelastic wave amplitude is a function of x, then

$$c = \frac{v}{v_r} < 1 \tag{14}$$

We neglect, from now on, viscous features of the vortex field, in view of their very weak influence on the propagation process; see [Cyrot and Pavuna 1992; Maruszewski et al. 2008].

Since the waves propagate along the layer, we should now take into account the proper boundary conditions for solving the set of equations (10). They follow from Figure 2, and read

$$h_y = 0 \quad \text{and} \quad \frac{du_y}{dx} = 0 \qquad \text{for } x = -1 \text{ and } x = 0. \tag{15}$$

The first of these conditions expresses the continuity of the tangent component of the magnetic field intensity, while the second follows from the equality $\sigma_{yz} = 0$ (the surfaces are free of loadings).

Substituting (11) into (15) we obtain the set of algebraic equations

$$\begin{aligned} -M(p_1, \Omega, c) S_1 e^{-p_1} + M(p_1, \Omega, c) S_2 e^{p_1} - M(p_2, \Omega, c) S_3 e^{-p_2} + M(p_2, \Omega, c) S_4 e^{p_2} &= 0, \\ S_1 p_1 e^{-p_1} - S_2 p_1 e^{p_1} + S_3 p_2 e^{-p_2} + S_4 p_2 e^{p_2} &= 0, \\ -M(p_1, \Omega, c) S_1 + M(p_1, \Omega, c) S_2 - M(p_2, \Omega, c) S_3 + M(p_2, \Omega, c) S_4 &= 0, \\ S_1 p_1 - S_2 p_1 + S_3 p_2 + S_4 p_2 &= 0, \end{aligned} \tag{16}$$

or

$$\boldsymbol{W} \cdot \boldsymbol{S} = \boldsymbol{0}, \tag{17}$$

where

$$\boldsymbol{S} = \{S_1, S_2, S_3, S_4\}^T. \tag{18}$$

Hence we arrive at the dispersion relation for SH magnetoelastic wave in the form

$$\det \boldsymbol{W} = 0. \tag{19}$$

A unique solution for (19) exists if

$$c = 1. \tag{20}$$

Thus the SH wave is nondispersive and its amplitude is independent of x. (See [Oliner 1978, Chapter 5].) So, the supposition (14) is no longer valid. But the final conclusion is such that we are dealing only with the plane SH wave mode in the vortex layer, which propagates with constant velocity — (20).

4. Compressional (C) and flexural (F) electromagnetoelastic waves

Let us now focus on electromagnetoelastic waves propagating along the magnetic vortex field layer. Our aim is to answer the question of whether they can be guided by such a layer. It is well known that, besides the SH magnetoelastc waves considered in the previous section, compressional (symmetric) and flexural (antisymmetric) waves may also propagate along waveguides in the form of a rod, plate or ribbon [Achenbach 1976, Chapter 8; Oliner 1978, Chapter 5; Eringen and Şuhubi 1975, Chapter 7] (Figure 3).

The solutions of the C and F wave equations (1) are looked this time for in the form (3) where $\tilde{f}(x_1)$ now stands for

$$\tilde{f}(x_1) = \{u_1, u_3, h_1, h_3, e_2\} \tag{21}$$

since (see Figure 4)

$$\boldsymbol{u} = [u_1, 0, u_3], \quad \boldsymbol{h} = [h_1, 0, h_3], \quad \boldsymbol{e} = [0, e_2, 0]. \tag{22}$$

On using now (21) and (5) in (1) the dimensionless F and C wave equations read

$$\begin{aligned}
\left(\tfrac{4}{3} + \tfrac{1}{3}\tilde{G}\right)u_{x,xx} + \Omega^2(1-c^2)u_x - \tfrac{1}{3}i\Omega c(\tilde{G}+1)u_{z,x} &= 0,\\
u_{z,xx} + \Omega^2\left[1 - c^2\left(\tfrac{4}{3} + \tfrac{1}{3}\tilde{G}\right)\right]u_z - \tfrac{1}{3}i\Omega c(\tilde{G}+1)u_{x,x} + i\tilde{\mu}H_0\Omega c h_x + \tilde{\mu}H_0 h_{z,x} &= 0,\\
\tilde{\lambda}_0^2 h_{x,xx} - (1 + \tilde{\lambda}_0^2\Omega^2 c^2)h_x + i\Omega c H_0 u_z &= 0,\\
\tilde{\lambda}_0^2 h_{z,zz} - (1 + \tilde{\lambda}_0^2\Omega^2 c^2)h_z + H_0 u_{z,x} &= 0,\\
\tilde{\lambda}_0^2 e_{y,xx} - (1 + \tilde{\lambda}_0^2\Omega^2 c^2)e_y - i\Omega c_1 H_0 u_z &= 0.
\end{aligned} \tag{23}$$

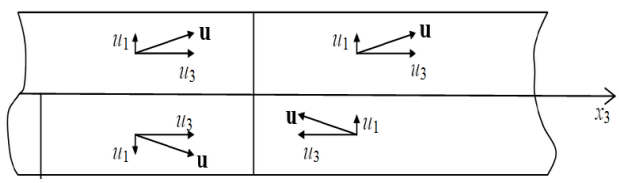

Figure 3. Symmetry of the vortex field displacements [Eringen and Şuhubi 1975]: symmetric-compressional wave (left pair) and antisymmetric-flexural wave (right pair).

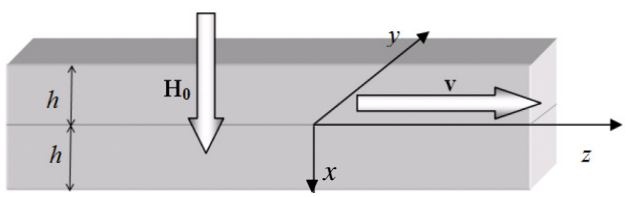

Figure 4. Geometry of the problem for the C and F waves in the vortex layer, following (5).

These equations should be completed by the electromagnetic field equations in vacuum:

$$h^p_{x,xx} - \Omega^2(c^2 - c_1^2)h^p_x = 0, \quad h^p_{z,xx} - \Omega^2(c^2 - c_1^2)h^p_z = 0, \quad e^p_{y,xx} - \Omega^2(c^2 - c_1^2)e^p_y = 0, \tag{24}$$

where superscript p denotes fields in a vacuum.

The jump and boundary conditions for (23) and (24) at the upper and lower planes of the layer read (see Figure 4)

$$\begin{gathered}
\sigma_{xx}|_{x=-1} = 0 \Longrightarrow \frac{du_x}{dx}|_{x=-1} = 0; \quad \sigma_{zx}|_{x=-1} = 0 \Longrightarrow \frac{du_z}{dx}|_{x=-1} = 0; \\
(h_x = h^p_x)|_{x=0} \text{ or } (e_y = e^p_y)|_{x=0}; \quad (h_z = h^p_z)|_{x=0}; \\
\sigma_{xx}|_{x=1} = 0 \Longrightarrow \frac{du_x}{dx}|_{x=1} = 0; \quad \sigma_{zx}|_{x=1} = 0 \Longrightarrow \frac{du_z}{dx}|_{x=1} = 0; \\
(h_x = h^p_x)|_{x=1} \text{ or } (e_y = e^p_y)|_{x=1}; \quad (h_z = h^p_z)|_{x=1}.
\end{gathered} \tag{25}$$

The desired C and F wave amplitudes are (using sh and ch to denote the hyperbolic sine and cosine)

$$\begin{aligned}
u_x &= P(\xi_2)S_4 \operatorname{ch}(\xi_2 x) + P(\xi_2)S_3 \operatorname{sh}(\xi_2 x) + P(\xi_3)S_6 \operatorname{ch}(\xi_3 x) + P(\xi_3)S_5 \operatorname{sh}(\xi_3 x) + P(\xi_4)S_8 \operatorname{ch}(\xi_4 x) \\
&\quad + P(\xi_4)S_7 \exp(\xi_4 x), \\
u_z &= Q(\xi_2)S_3 \operatorname{ch}(\xi_2 x) + Q(\xi_2)S_4 \operatorname{sh}(\xi_2 x) + Q(\xi_3)S_5 \operatorname{ch}(\xi_3 x) + Q(\xi_3)S_6 \operatorname{sh}(\xi_3 x) + Q(\xi_4)S_7 \operatorname{ch}(\xi_4 x) \\
&\quad + Q(\xi_4)S_8 \operatorname{sh}(\xi_4 x), \\
h_x &= S_3 \operatorname{ch}(\xi_2 x) + S_4 \operatorname{sh}(\xi_2 x) + S_5 \operatorname{ch}(\xi_3 x) + S_6 \operatorname{sh}(\xi_3 x) + S_7 \operatorname{ch}(\xi_4 x) + S_8 \operatorname{sh}(\xi_4 x), \\
h_z &= -\frac{i}{\Omega c}[\xi_2 S_4 \operatorname{ch}(\xi_2 x) + \xi_2 S_3 \operatorname{sh}(\xi_2 x) + \xi_3 S_6 \operatorname{ch}(\xi_3 x) + \xi_3 S_5 \operatorname{sh}(\xi_3 x) + \xi_4 S_8 \operatorname{ch}(\xi_4 x) + \xi_4 S_7 \operatorname{sh}(\xi_4 x)], \\
e_y &= -\frac{c_1}{c}[S_3 \operatorname{ch}(\xi_2 x) + S_4 \operatorname{sh}(\xi_2 x) + S_5 \operatorname{ch}(\xi_3 x) + S_6 \operatorname{sh}(\xi_3 x) + S_7 \operatorname{ch}(\xi_4 x) + S_8 \operatorname{sh}(\xi_4 x)],
\end{aligned} \tag{26}$$

where

$$P(\xi) = -\frac{\xi(\tilde{G}+1)(\tilde{\lambda}_0^2\xi^2 - 1 - \tilde{\lambda}_0^2\Omega^2c^2)}{H_0[(4+\tilde{G})\xi^2 + 3\Omega^2(1-c^2)]}, \quad Q(\xi) = i\frac{\tilde{\lambda}_0^2\xi^2 - 1 - \tilde{\lambda}_0^2\Omega^2c^2}{\Omega c H_0}.$$

The parameters ξ_m are the solutions of the characteristic equation

$$(A\xi^6 + B\xi^4 + C\xi^2 + D)(\Omega^2c^2\tilde{\lambda}_0^2 - \tilde{\lambda}_0^2\xi^2 + 1) = 0, \tag{27}$$

whose coefficients A, B, C and D are given in the Appendix.

The amplitudes of the electromagnetic waves outside the layer read as follows:

– above the upper plane:

$$h^p_x = S_1[\operatorname{ch}(\tilde{\xi}_1 x) + \operatorname{sh}(\tilde{\xi}_1 x)], \quad h^p_z = -\frac{i\tilde{\xi}_1}{\Omega c}S_1[\operatorname{ch}(\tilde{\xi}_1 x) + \operatorname{sh}(\tilde{\xi}_1 x)], \quad e^p_y = -\frac{c_1}{c}S_1[\operatorname{ch}(\tilde{\xi}_1 x) + \operatorname{sh}(\tilde{\xi}_1 x)], \tag{28}$$

– below the lower plane:

$$h^p_x = S_2[\operatorname{ch}(\tilde{\xi}_1 x) - \operatorname{sh}(\tilde{\xi}_1 x)], \quad h^p_z = \frac{i\tilde{\xi}_1}{\Omega c}S_2[\operatorname{ch}(\tilde{\xi}_1 x) - \operatorname{sh}(\tilde{\xi}_1 x)], \quad e^p_y = -\frac{c_1}{c}S_2[\operatorname{ch}(\tilde{\xi}_1 x) + \operatorname{sh}(\tilde{\xi}_1 x)]. \tag{29}$$

Now using solutions (26), (28) and (29) in the boundary and jump conditions (25) we get a set of eight algebraic equations for S_1 through S_8. They are given in the Appendix. After laborious calculations this set of eight equation splits into two uncoupled sets:

$$\boldsymbol{W}_C \cdot \boldsymbol{S}_C = \boldsymbol{0}, \tag{30}$$

$$\boldsymbol{W}_F \cdot \boldsymbol{S}_F = \boldsymbol{0}, \tag{31}$$

where

$$\boldsymbol{S}_C = \left\{\tfrac{1}{2}(S_1 - S_2),\, S_4,\, S_6,\, S_8\right\}^T, \quad \boldsymbol{S}_C = \left\{\tfrac{1}{2}(S_1 + S_2),\, S_3,\, S_5,\, S_7\right\}^T.$$

Hence the dispersion relations for the considered waves are

– for compressional modes: $\det \boldsymbol{W}_C = 0,$ (32)

– for flexural modes: $\det \boldsymbol{W}_F = 0.$ (33)

5. Numerical results

In this section we limit ourselves to the numerical analysis of the compressional and flexural electromagnetic wave propagation conditions since the SH magnetic wave is nondispersive propagating with the constant velocity and is amplitude independent of the thickness of the layer. All the calculations have been made for $YBa_2Cu_3O_{6+x}$, or YBCO, ceramics. We have restricted ourselves to the *lattice-like* state of the vortex field, so the external magnetic H_0 is taken slightly higher than the limiting lower magnetic field value H_{c1}.

Firstly, let us take care of the existence of the C and F waves in the layer. The conditions dealing with their existence result from characteristic equation (27). That situation is illustrated in Figure 5.

Before we start analysis of the amplitude distribution of the C and F waves in the layer we should consider their dispersion. Figure 6 shows the dispersion of the C waves calculated from (32), and the F waves, from (33).

Remark that both in the C and F wave cases only one single modes propagate. That feature is anomalous and differs from that for the classical elastic body where infinite number of modes propagate [Eringen and Şuhubi 1975, Chapter 7]. From Figure 6 it is also visible that waves C and F characterize anomalous dispersion: they propagate with acoustic velocity having optical frequencies (C wave has

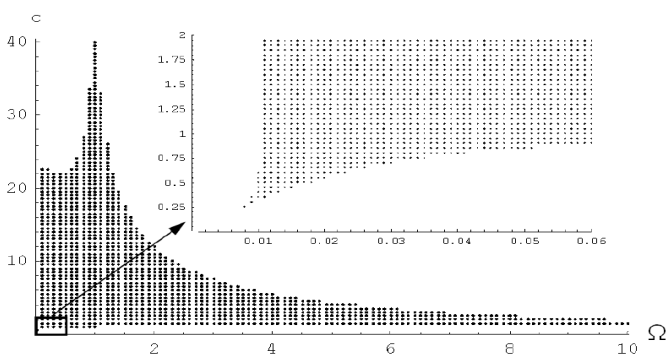

Figure 5. Area of existence of C and F waves.

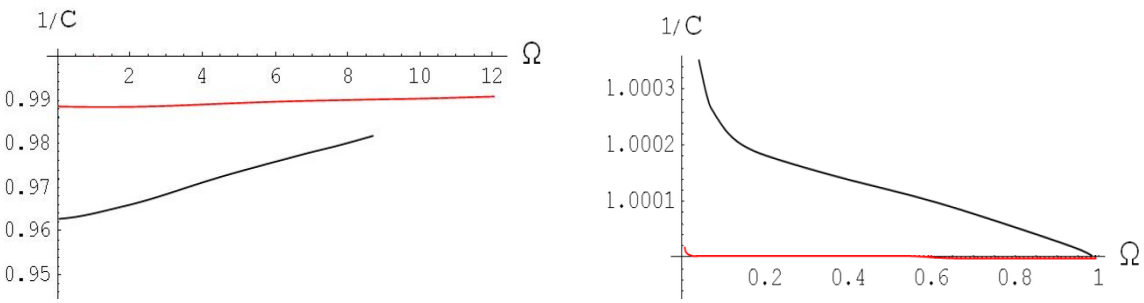

Figure 6. Dispersion of C waves (left) and of F waves (right) for $h = 10^{-7}$ m. Black: $H_0 = 1$; red: $H_0 = 10$.

higher frequency comparable to the frequency spectrum of the visible light then F wave has lower frequency comparable to the frequency spectrum of the infrared rays). Moreover, for both cases the dispersion decreases if the external magnetic field H_0 increases. Now let us take care of the amplitudes.

Compressional waves. The compressional (C) wave amplitudes for h_x, h_z, e_y, u_x, u_z, σ_{xx} and σ_{xz} are presented in Figure 7. Shaded areas indicate the layer region.

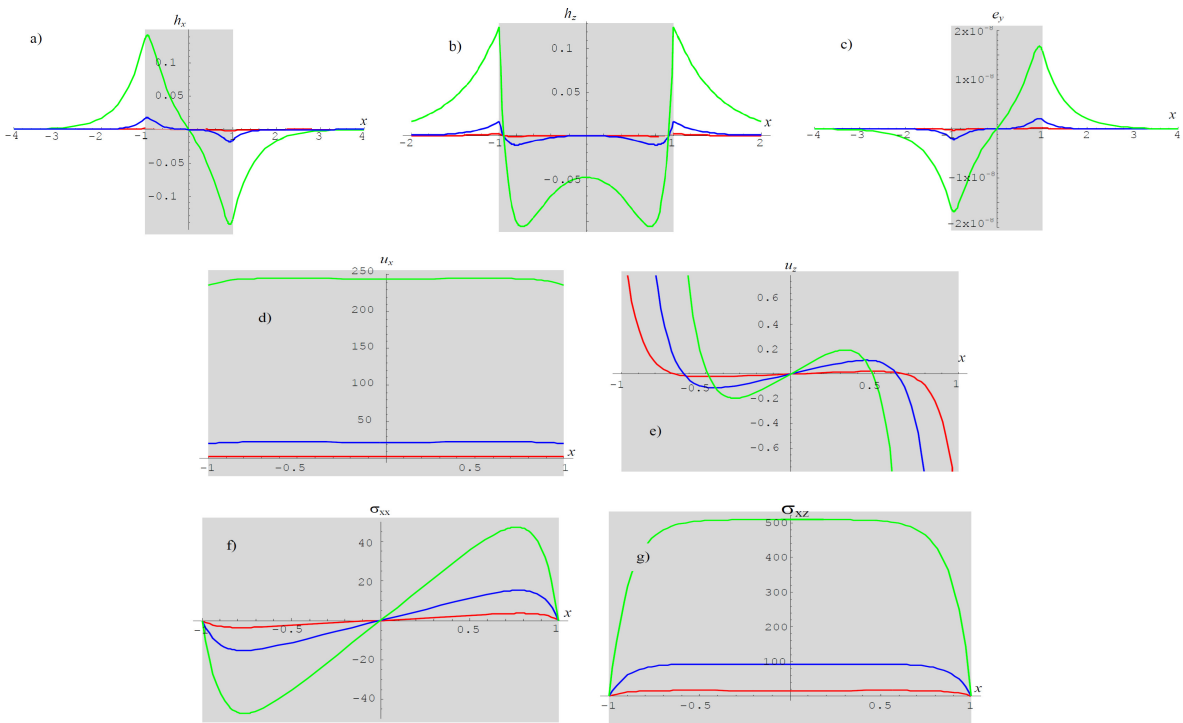

Figure 7. Compressional wave amplitudes for $H_0 = 1$ and $h = 10^{-7}$ m. Top row: h_x, h_z, e_y. Middle row: u_x, u_z. Bottom row: σ_{xx}, σ_{xz}. Green: $\Omega = 0.2$. Blue: $\Omega = 0.6$. Red: $\Omega = 0.9$.

The simple look at the drawings in Figure 7 shows that in the case of the electromagnetic part of the C waves (top row) their amplitudes reach extremal values at the lateral planes of the layer and are continuous across them. But the mechanical part of the C waves behave differently (middle and bottom rows). They naturally exist only between the lateral planes of the layer. Then the longitudinal u_x and shear σ_{xz} modes are symmetric with respect to the middle surface of the layer. But the general conclusion for all modes is such that all their amplitudes decreases if the frequency Ω increases.

Flexural waves. The flexural (F) wave amplitudes for $h_x, h_z, e_y, u_x, u_z, \sigma_{xx}$ and σ_{xz} are presented in Figure 8.

The properties of the F wave amplitudes differ from their C counterpart. For example, h_x and e_z amplitudes are extremal at the middle surface of the layer and do not "feel" its lateral planes disappearing smoothly in infinity. Then antisymmetric h_z is extremal at the above planes. The mechanical mode amplitudes behave as follows:

– u_x mode is linear and antisymmetric vanishing at the middle surface; it exist solely inside the layer.

– u_z is symmetric with respect to the middle surface reaching there extremum.

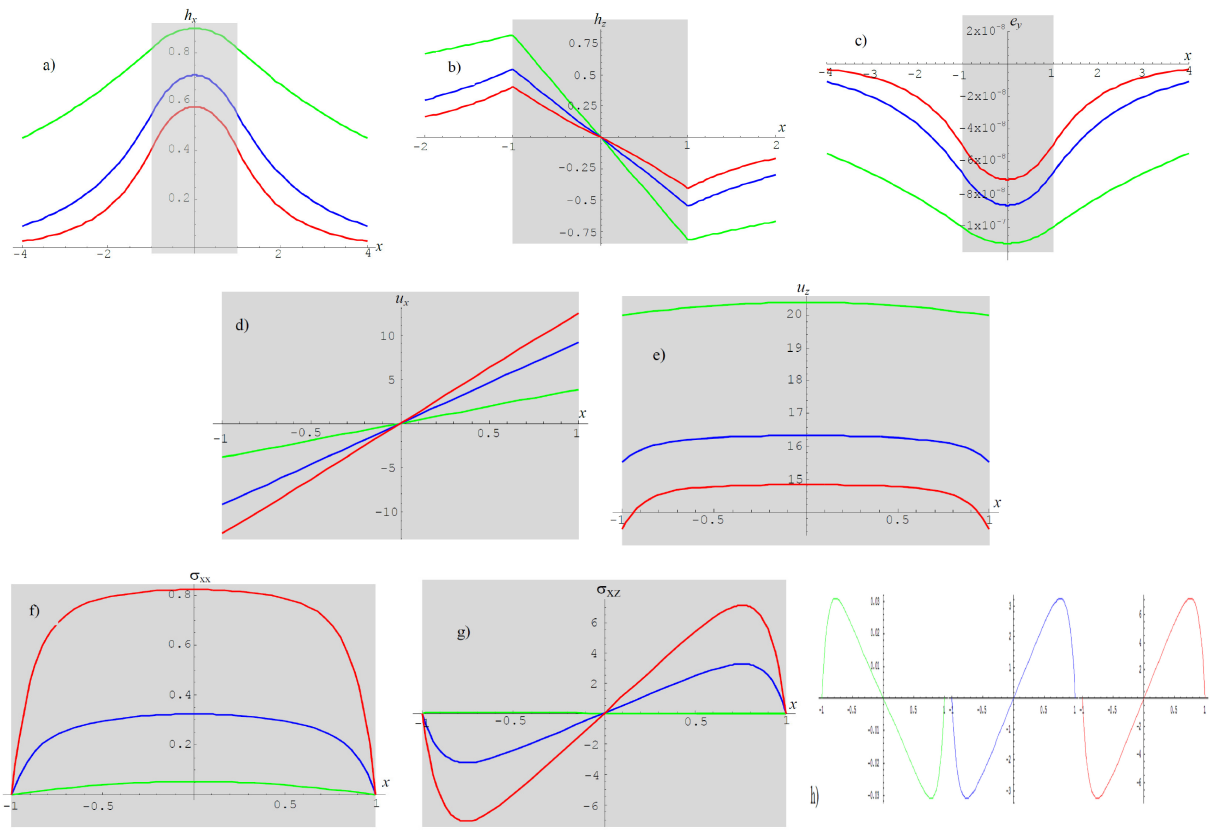

Figure 8. Flexural wave amplitudes for $H_0 = 1$ and $h = 10^{-7}$ m. Green: $\Omega = 0.2$. Blue: $\Omega = 0.6$. Red: $\Omega = 0.9$. Top row: h_x, h_z, e_y. Middle row: u_x, u_z. Bottom row: σ_{xx}, σ_{xz}. The last panel, (h), shows the same graphs as (g) but at different scales.

– σ_{xx} (the trace part of the stress associated with the wave propagation direction) behaves like u_z; however, it vanish at the lateral planes.

– σ_{xz} is antisymmetric with respect to the middle plane vanishing at the lateral surfaces. However it behaves anomalously; from the last two panels in the bottom row of Figure 8 we see that there exists a frequency Ω_{cr} for which σ_{xz} values are equal to zero across the layer, so the σ_{xz} stress values change sign if they are observed for $\Omega < \Omega_{cr}$ or for $\Omega > \Omega_{cr}$.

According to the dependence of Ω the electromagnetic mode amplitudes decrease if the frequency Ω increases contrary to the mechanical modes behavior (Figure 8).

6. Conclusions

The considerations made in the paper show that two general types of waves can propagate in the vortex array existing solely in the superconducting layer. The first one deals with the SH magnetoelastic modes and the second type concerns electromagnetoelastic compressional and flexural modes. It is known that layers can be used in some situations as waveguides. Investigations made in the paper confirmed that guided signal transmission along the magnetic vortex field is possible. Natural conditions for such an application exist in free space, so such a technology, which is not energy consuming, might be used in space ships or other similar equipment.

Except for classical properties, electromagnetoelastic C and F waves involve the same anomalous features, as seen in Figure 8(c), (g), (h). The u_x mode is linearly distributed across the layer, which differs from the classical (mechanical non-vortex) situation. But a much more interesting result is presented in Figure 8 (g), (h). We see that there exists a definite critical frequency Ω_{cr} for which the amplitude of the F σ_{xz} mode vanishes across the entire layer. That means that for such critical frequency $\Omega_{cr}\sigma_{xz}$ mode does not propagate.

Appendix: The coefficients of (27) and the algebraic equations encoded in (30)–(31)

The coefficients of (27) are given by

$$
\begin{aligned}
A &= \tilde{\lambda}_0^2(4+\tilde{G}),\\
B &= -4(3\Omega^2c^2\tilde{\lambda}_0^2+1)-\tilde{G}(3\Omega^2c^2\tilde{\lambda}_0^2+1)-4H_0^2\tilde{\mu}+7\Omega^2\tilde{\lambda}_0^2+\tilde{G}(\Omega^2\tilde{\lambda}_0^2-H_0^2\tilde{\mu}),\\
C &= 4\Omega^2c^2(3\Omega^2c^2\tilde{\lambda}_0^2+2)+\Omega^2[\tilde{G}c^2(3\Omega^2c^2\tilde{\lambda}_0^2+2)+7(H_0^2c^2\tilde{\mu}-2\Omega^2c^2\tilde{\lambda}_0^2-1)]\\
&\quad +\Omega^2[\tilde{G}(H_0^2c^2\tilde{\mu}-2\Omega^2c^2\tilde{\lambda}_0^2-1)-3(H_0^2\tilde{\mu}-\Omega\tilde{\lambda}_0^2)],\\
D &= -4\Omega^2c^4(\Omega^2c^2\tilde{\lambda}_0^2+1)-\Omega^4c^2[\tilde{G}c^2(\Omega^2c^2\tilde{\lambda}_0^2+1)+3H_0^2c^2\tilde{\mu}-7(\Omega^2c^2\tilde{\lambda}_0^2+1)]\\
&\quad +\Omega^4[\tilde{G}c^2(\Omega^2c^2\tilde{\lambda}_0^2+1)+3(H_0^2c^2\tilde{\mu}-\Omega^2c^2\tilde{\lambda}_0^2-1)].
\end{aligned}
$$

We next give the algebraic equations satisfied for $S_1, S_2, \ldots, S_8$. Let

$$
Y(\xi)=\tfrac{1}{3}(4+\tilde{G})P(\xi)\xi-\tfrac{1}{3}i\Omega c(\tilde{G}-2)Q(\xi) \quad \text{and} \quad Z(\xi)=[-Q(\xi)\xi+i\Omega cP(\xi)],
$$

where sh and ch denote the hyperbolic sine and cosine. Then

$$
\begin{aligned}
Y(\xi_2)\,\mathrm{ch}\,\xi_2\,S_3 - Y(\xi_2)\,\mathrm{sh}\,\xi_2\,S_4 + Y(\xi_3)\,\mathrm{ch}\,\xi_3\,S_5 - Y(\xi_3)\,\mathrm{sh}\,\xi_3\,S_6 + Y(\xi_4)\,\mathrm{ch}\,\xi_4\,S_7 - Y(\xi_4)\,\mathrm{sh}\,\xi_4\,S_8 &= 0,\\
Z(\xi_2)\,\mathrm{ch}\,\xi_2\,S_3 - Z(\xi_2)\,\mathrm{sh}\,\xi_2\,S_4 + Z(\xi_3)\,\mathrm{ch}\,\xi_3\,S_5 - Z(\xi_3)\,\mathrm{sh}\,\xi_3\,S_6 + Z(\xi_4)\,\mathrm{ch}\,\xi_4\,S_7 - Z(\xi_4)\,\mathrm{sh}\,\xi_4\,S_8 &= 0,\\
\tilde{\xi}_1(\mathrm{ch}\,\tilde{\xi}_1 - \mathrm{sh}\,\tilde{\xi}_1)S_1 + \xi_2\,\mathrm{sh}\,\xi_2\,S_3 - \xi_2\,\mathrm{ch}\,\xi_2\,S_4 - \xi_3\,\mathrm{sh}\,\xi_3\,S_5 - \xi_3\,\mathrm{ch}\,\xi_3\,S_6 + \xi_4\,\mathrm{sh}\,\xi_4\,S_7 - \xi_4\,\mathrm{ch}\,\xi_4\,S_8 &= 0,\\
(\mathrm{ch}\,\tilde{\xi}_1 - \mathrm{sh}\,\tilde{\xi}_1)S_1 - \mathrm{ch}\,\xi_2\,S_3 + \mathrm{sh}\,\xi_2\,S_4 - \mathrm{ch}\,\xi_3\,S_5 + \mathrm{sh}\,\xi_3\,S_6 - \mathrm{ch}\,\xi_4\,S_7 + \mathrm{sh}\,\xi_4\,S_8 &= 0,\\
Y(\xi_2)\,\mathrm{ch}\,\xi_2\,S_3 + Y(\xi_2)\,\mathrm{sh}\,\xi_2\,S_4 + Y(\xi_3)\,\mathrm{ch}\,\xi_3\,S_5 + Y(\xi_3)\,\mathrm{sh}\,\xi_3\,S_6 + Y(\xi_4)\,\mathrm{ch}\,\xi_4\,S_7 + Y(\xi_4)\,\mathrm{sh}\,\xi_4\,S_8 &= 0,\\
Z(\xi_2)\,\mathrm{ch}\,\xi_2\,S_3 + Z(\xi_2)\,\mathrm{sh}\,\xi_2\,S_4 + Z(\xi_3)\,\mathrm{ch}\,\xi_3\,S_5 + Z(\xi_3)\,\mathrm{sh}\,\xi_3\,S_6 + Z(\xi_4)\,\mathrm{ch}\,\xi_4\,S_7 + Z(\xi_4)\,\mathrm{sh}\,\xi_4\,S_8 &= 0,\\
\tilde{\xi}_1(\mathrm{ch}\,\tilde{\xi}_1 - \mathrm{sh}\,\tilde{\xi}_1)S_2 + \xi_2\,\mathrm{sh}\,\xi_2\,S_3 + \xi_2\,\mathrm{ch}\,\xi_2\,S_4 + \xi_3\,\mathrm{sh}\,\xi_3\,S_5 + \xi_3\,\mathrm{ch}\,\xi_3\,S_6 + \xi_4\,\mathrm{sh}\,\xi_4\,S_7 + \xi_4\,\mathrm{ch}\,\xi_4\,S_8 &= 0,\\
(\mathrm{ch}\,\tilde{\xi}_1 - \mathrm{sh}\,\tilde{\xi}_1)S_2 - \mathrm{ch}\,\xi_2\,S_3 - \mathrm{sh}\,\xi_2\,S_4 - \mathrm{ch}\,\xi_3\,S_5 - \mathrm{sh}\,\xi_3\,S_6 - \mathrm{ch}\,\xi_4\,S_7 - \mathrm{sh}\,\xi_4\,S_8 &= 0.
\end{aligned}
$$

References

[Achenbach 1976] J. Achenbach, *Wave propagation in elastic solids*, North-Holland, Amsterdam, 1976.

[Blatter et al. 1994] G. Blatter, M. V. Feigelman, V. B. Geshkenbein, A. L. Larkin, and V. M. Vinokur, "Vortices in high-temperature superconductors", *Rev. Mod. Phys.* **66** (1994), 1125–1388.

[Brandt 1995] E. H. Brandt, "The flux-line lattice in superconductors", *Rep. Prog. Phys.* **58** (1995), 1465–1594.

[Cyrot and Pavuna 1992] M. Cyrot and D. Pavuna, *Introduction to superconductivity and high-T_c materials*, World Scientific, Singapore, 1992.

[Eringen and Şuhubi 1975] A. C. Eringen and E. S. Şuhubi, *Elastodynamics*, vol. 2, Academic Press, New York, 1975.

[Maruszewski 1998] B. T. Maruszewski, "Superconducting fullerenes in a nonconventional thermodynamical model", *Arch. Mech.* **50** (1998), 497–508.

[Maruszewski 2007] B. T. Maruszewski, "On a nonclassical thermoviscomechanical stress in the vortex field in the type-II superconductor", *Phys. Stat. Sol. B* **24** (2007), 919–927.

[Maruszewski et al. 2007] B. T. Maruszewski, A. Drzewiecki, and R. Starosta, "Anomalous features of the thermomagnetoelastic field in a vortex array in a superconductor: propagation of Love's waves", *J. Thermal Stresses* **30** (2007), 1049–1065.

[Maruszewski et al. 2008] B. T. Maruszewski, A. Drzewiecki, and R. Starosta, "Propagation of a surface wave in a vortex array along a superconducting heterostructure", *J. Mech. Mat. Struct.* **3** (2008), 1097–1104.

[Oliner 1978] A. A. Oliner, *Waveguides for acoustic surface waves*, edited by A. A. Oliner, Springer, New York, 1978.

Received 24 Jan 2011. Revised 25 Oct 2011. Accepted 13 Jan 2012.

BOGDAN T. MARUSZEWSKI: bogdan.maruszewski@put.poznan.pl
Institute of Applied Mechanics, Poznan University of Technology, ul. Jana Pawla II 24, 60-965 Poznan, Poland

ANDRZEJ DRZEWIECKI: andrzej.drzewiecki@put.poznan.pl
Institute of Applied Mechanics, Poznan University of Technology, ul. Jana Pawla II 24, 60-965 Poznan, Poland

ROMAN STAROSTA: roman.starosta@put.poznan.pl
Institute of Applied Mechanics, Poznan University of Technology, ul. Jana Pawla II 24, 60-965 Poznan, Poland

JOURNAL OF MECHANICS OF MATERIALS AND STRUCTURES

jomms.net

Founded by Charles R. Steele and Marie-Louise Steele

See http://jomms.net for submission guidelines.

JoMMS (ISSN 1559-3959) is published in 10 issues a year. The subscription price for 2012 is US $555/year for the electronic version, and $735/year (+$60 shipping outside the US) for print and electronic. Subscriptions, requests for back issues, and changes of address should be sent to Mathematical Sciences Publishers, Department of Mathematics, University of California, Berkeley, CA 94720–3840.

JoMMS peer-review and production is managed by EditFLOW® from Mathematical Sciences Publishers.

PUBLISHED BY

mathematical sciences publishers

http://msp.org/

A NON-PROFIT CORPORATION

Typeset in LaTeX

Journal of Mechanics of Materials and Structures

Volume 7, No. 3 March 2012

Special issue

Trends in Continuum Physics (TRECOP 2010)